Nuclear Mathematical and Computational Sciences: A Century in Review, A Century Anew
Gatlinburg, Tennessee, April 6-11, 2003, on CD-ROM, American Nuclear Society, LaGrange Park, IL (2003)

FAST REACTOR BULK SHIELDING EXPERIMENTS FOR VALIDATION OF SHIELDING COMPUTATIONAL TECHNIQUES

Indira.R and Sunilkumar.D
Reactor Physics Division
Indira Gandhi Center for Atomic Research
Kalpakkam 603 102, India
indira@igcar.ernet.in

Dravid H.K and Rasheed.K.K
Reactor Physics Design Division
Bhabha Atomic Research Centre
Trombay, Mumbai 400 022, India
dravid@magnum.barc.ernet.in

ABSTRACT

Fast Reactor shielding experiments are carried out in shielding corner facility of APSARA reactor, to assess the overall accuracy of the codes and nuclear data used in fast reactor shield design. As APSARA is a swimming pool-type thermal reactor, typical fast reactor shielding facility was created by using uranium assemblies as spectrum converter. The flux was also enhanced by replacing water by air. Experiments have been carried out to study the neutron attenuation through typical fast reactor radial and axial bulk shielding materials such as steel, sodium, graphite, borated graphite and boron carbide. Large number of reaction rates sensitive to different regions of the neutron energy spectrum, were measured using foil activation and SSNTD techniques. The measured neutron spectrum on the incident face of shield model compares well with the calculated fast reactor blanket leakage neutron spectrum These experiments were analysed using discrete ordinate transport codes with multigroup cross section sets. Comparison of measured reaction rates with calculations provided suitable bias factors for parameters relevant to shield design. Comparison indicates that the calculated reaction rates within the shield model suffer from considerable uncertainties, in shield models with boron carbide/ borated graphite.

Key Words: fast reactor shielding, mockup experiments, transport codes, multigroup cross sections, validation.

1. INTRODUCTION

In a pool type sodium cooled fast reactor, the core consisting of fissile material is surrounded by a blanket of fertile material and invessel shielding, The intermediate heat exchangers (IHX) and sodium pumps are also located in the pool of sodium. The invessel shielding serves the purpose

of reducing the neutron flux such that, the radiation damage to the inner vessel, secondary sodium activation in the IHX and the activation of IHX and pump, are within permissible limits.

The neutron transport through shields is described by the well known linear Boltzmann transport equation. The neutron flux incident on the invessel shield is of the order of 10^{13} n/cm^2/s. The incident neutron spectrum is also very hard with negliglible thermal component. The calculations span an energy range of 0.025 eV to 14 MeV and attenuation through more than 40 mean free paths of shield thickness. As the source is limited to the core-blanket region, the neutron flux has anisotropic angular distribution. Hence the shield design calculations involve accurate estimation of the neutron flux spectrum at locations deep into the shield. For these *deep penetration* problems, the transport equation is not amenable to analytic solutions and is formidable even in the case of numerical solutions [1].

The most widely used deterministic method for solving neutron transport equation for shielding problems, is the finite-difference, discrete ordinate (DSN) technique. In this technique, space variables and angle variables are discretised. The energy variable is also discretised into a large number of energy groups. The most commonly used codes employing this technique are the one-dimensional (1-D) transport code ANISN and 2-dimensional (2-D) transport code DORT. The cross sections for processes such as absorption, scattering etc., which are available as point cross section data as a function of neutron energy, are processed to obtain multigroup cross section sets. Typical multigroup cross section set used by us is 100 group neutron cross section set DLC-2. The transport calculations are sensitive to uncertainties in cross section data. For example, in a calculation of transport through 10 mfp thick shield, 1% error in total cross section in one of the dominating groups can lead to 50% error in total transmitted flux [2].

A large number of benchmark analyses are carried out to assess the uncertainties due to cross section data and numerical methods [3]. To validate cross section data, a large number of integral experiments have been carried out in USA at Tower Shielding Facility in ORNL, to study transmission through iron, sodium and steel [4]. In France, similar JASON experimental program was undertaken in the HARMONIE fast flux test facility, for studies of transmission through sodium, steel and boron carbide [5]. The European countries participating in EFR (European Fast Reactor) undertook the JANUS programme in the ASPIS shielding facility at AEA, Winfrith, UK, for studies of transmission through steel, sodium and boron carbide [6]. The Japanese have conducted FBR shielding mockup experiments in colloboration with USA at Tower Shielding Facility in ORNL, under JASPER programme [7]. Transmission through steel, sodium, graphite and boron carbide were studied. Apart from these, mockup experiments are carried out prior to detailed shield design for the proposed shield configuration in reactor, to obtain bias factors and to optimise the shield. In these mockup experiments, a large number of reaction rates sensitive to different regions of the neutron energy spectrum, are measured. The ratios of measured to calculated reaction rates corresponding to the parameters of interest are called the bias factors.

The in-vessel radial shield configurations of Prototype Fast Breeder Reactor (PFBR), being designed at IGCAR, Kalpakkam, consist of stainless steel ,borated graphite/ boron carbide and sodium. As shield thickness has a direct implication on the size of the inner vessel and reactor vessel, a cost effective design calls for optimisation of shields. The design calculations are

normally carried out using deterministic methods, employing discrete ordinate techniques. 1-dimensional (1-D) and 2-dimensional (2-D) transport codes with multigroup cross section sets. To assess the overall accuracy of the codes and nuclear data, all the shielding benchmark problems in ORNL-RSIC-25 were analysed [8]. ORNL benchmark experiment on neutron transport through thick sodium was analysed [9]. However, to obtain bias factors for specific shield configuration, mock-up experiments have to be carried out in shielding facilities. To obtain the bias factors for PFBR shield design, mockup experiments have been carried out in Apsara Reactor at BARC, jointly by IGCAR and BARC [10].

Apsara reactor is a 1 MWt swimming pool light water reactor with a shielding corner facility. It has a unique movable core assembly of enriched Uranium- Aluminium alloy. The neutron flux level of $\sim 10^7$ n/cm^2/s in the shielding corner was inadequate for the purpose of carrying out experiments on neutron transport through thick shields. The reason for this low flux is the presence of about 40 cm of water between core and the pool-wall. The neutron flux level was enhanced to 1.03×10^{10} n/cm^2/s by displacing most of the water between the core edge and stainless steel (SS) liner of APSARA pool on the shielding corner-side with an air-filled aluminum box. The energy spectrum of neutrons in the shielding corner is essentially a thermal reactor neutron spectrum. Converter assemblies (CA) made of depleted uranium, were placed in a trolley close to the Al-panel in the shielding corner, such that the emergent neutron spectrum represents PFBR blanket leakage neutron spectrum**.**

Experiments have been carried out in the shielding corner cavity of Apsara to study the neutron attenuation through shielding materials such as steel, sodium, graphite, borated graphite and boron carbide. Six sets of experiments to study neutron attenuation in radial shields and one with axial shield of graphite and steel, have been completed. Three radiation streaming experiments are also being carried out. Calculations for the various shield configurations have been carried out using 2D transport code DORT[11] and DLC-2 library[12]. Analysis of reaction rates have been carried out and the ratio of calculated reaction rate (C) to the experimentally measured value (E) have been obtained.

2. DETAILS OF FAST REACTOR SHIELDING FACILITY

Apsara reactor is a 1 MWt swimming pool light water reactor with a shielding corner facility. It has a unique movable core assembly of enriched Uranium- Aluminium alloy and can be operated in four positions A, B, C and C' (Fig.1). To facilitate measurements in shielding corner, the reactor is operated at C' position, closest to shielding corner. During access to shielding corner, the core is moved away to A position. The shielding corner consists of three trolleys (with Block-1, Block-2 and Block-3 concrete shields) mounted on wheels, which can be moved on rails (Fig.1). The measurements are carried out in the cave of Block-3.

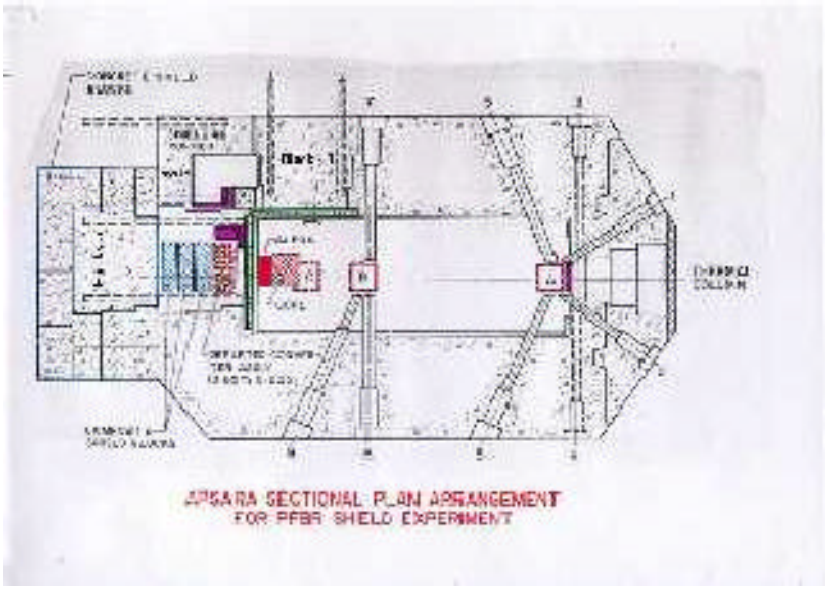

Figure.1 Sectional Plan of APSARA Reactor

In order to increase the neutron flux at shielding corner water from the gap between the core and the SS liner towards block-3 is displaced using an aluminium box. The air cavity in the box is 31.5 cm. The APSARA core edge neutron spectrum (mostly thermal) is converted to a typical hard PFBR blanket leakage neutron spectrum using converter assemblies mounted on a trolley. This trolley is positioned outside the reactor pool in the cave of block-3.

The converter assembly (CA) region consists of an arrangement of depleted Uranium assemblies in 4 rows, with 9 and 8 subassemblies in alternate rows. The converter subassemblies are placed on a trolley fabricated specially for this purpose. 34 converter assemblies (CA) are loaded on to the positions provided on the top plate of the trolley.

Figure.2 Plan View of Shielding Corner in APSARA

Behind the converter assemblies, shield models are placed on shield model trolley. For installation of shield models, trolley with Block-1 concrete is moved out and the shield model trolley is pulled out. After installation of shield models on the trolley, it is pushed back into the cave and trolley with block-1 is returned to its original position. This way the whole arrangement is housed in block 3 of shielding corner. Fig.2 shows the plan view of the experimental arrangement in the shielding corner. Biological shields around shielding corner are reinforced to ensure that the increased dose rates due to replacement of water by air, activation of converter assemblies and shield models are brought down to permissible limits. Installation and removal of detectors in shield models is carried out from foil retrieval location in hollow space of Block-2. Entry to this location is effected by pulling out Block-3. Dose rate at foil retrieval location is minimized by suitable placement of shielding around CA and near the mouth of foil retrieval location in shielding corner. Plan view of the experimental arrangement in shielding corner with foil retrieval location is shown in Fig.3.

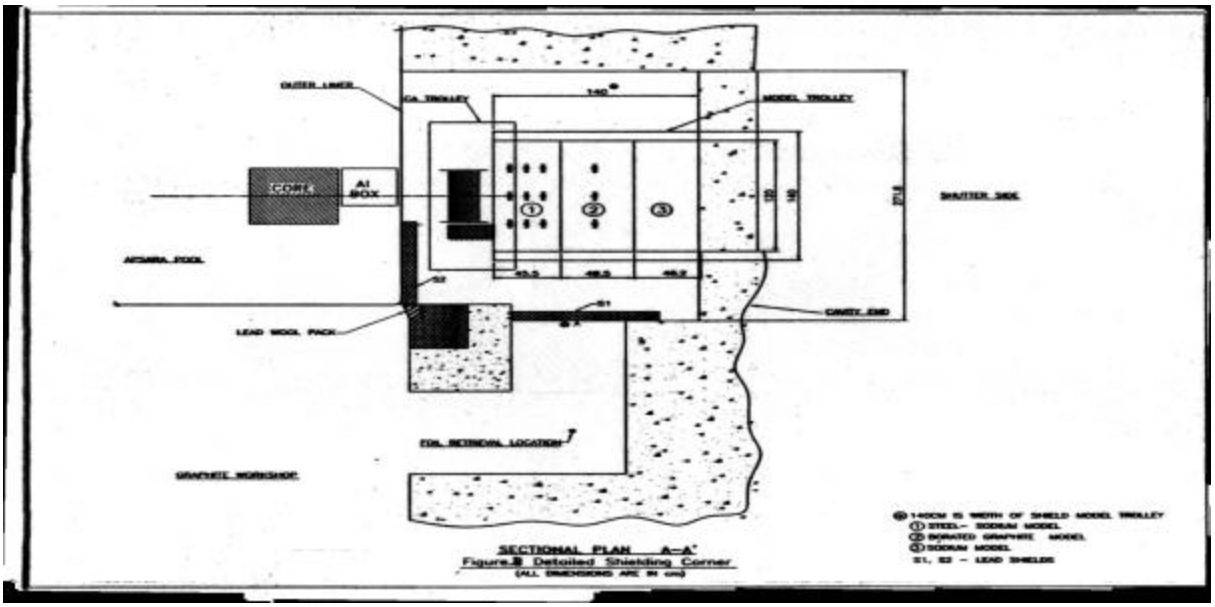

Figure 3. Plan View of Experimental Arrangement in Shielding Corner

3. MEASUREMENTS

The experiments involve a large neutron flux attenuation and measurement of neutron spectrum on the incident face. Hence, large number of activation detectors such as gold, sodium, copper, nickel, indium, iron, titanium and sulfur were used. The detectors used cover the entire energy range from thermal (0.025 eV) to 14 MeV. Gold foils (bare and Cd-covered) are a good measure of thermal and epithermal neutron flux mainly in eV range. As sodium activity is an important parameter in design, it is directly measured with the help of bare and cadmium covered sodium foils. Neptunium and Indium reaction rates (essentially due to neutrons of energy above ≈0.4 MeV and ≈1 MeV respectively) provide data related to radiation damage fluence (dpa). Nickel and Sulphur foil (threshold activation) reaction rates are used to obtain very hard energy component (> 2.5 MeV) of fast neutron flux. Solid State nuclear track detectors (SSNTD) were used to get fission reaction rates for Neptunium, Thorium and natural Uranium.

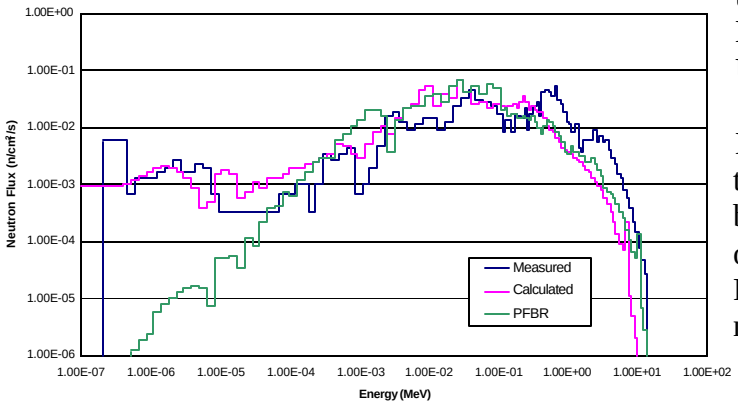

Detailed incident neutron spectrum on the emergent face of CA was measured by unfolding the measured reaction rates of a large number of activation detectors. Fig.4 gives a comparison of the measured neutron spectrum on the emergent face of CA with the calculated blanket leakage neutron spectrum of PFBR [13]. This shows that comparison is very good over the energy range of interest (E>100 eV).

Figure 4. Comparison of Measured and Calculated Neutron Spectrum with PFBR Blanket Exit Spectrum

For the experimental campaign, ten laminar shield models were fabricated. Two models of 455 mm thickness, are of sodium-carbon steel (CS) with different volume fractions, the third shield model is a borated graphite -CS-sodium model, the fourth shield model is a 462 mm thick sodium model and the fifth is a 495 mm thick boron carbide – CS- sodium model. The sixth and seventh shield models are variations of fifth model, wherein, some of the boron carbide is replaced with graphite. The volume fractions in the model are close to the volume fractions in radial shield configuration of PFBR. The eighth, ninth and tenth models of steel- sodium and graphite, of thickness 46.5 cm, 40.6 cm and 29.5 cm respectively, simulate the axial shielding in PFBR. Vertical slots are provided at several locations in each of these models for inserting specially fabricated SS foil-holders with activation foil detectors and SSNTDs. A telescopic foil retriever was used for installation and retrieval of foil holders after irradiation.

The first two experiments were carried out to study neutron transport through sodium-steel with two different volume fractions. The third and the fourth experiments were carried out to study neutron transport through sodium-steel- borated graphite and sodium-steel-boron carbide materials. In the fifth and sixth experiments, progressive replacement of boron carbide in the fourth experiment by graphite was studied. The seventh experiment for simulating axial shield was carried out with sodium-steel-graphite shield models. In this experiment, U-235 fission rate and B-10(n,α) reaction rates were also measured, to study the effectiveness of the neutron monitoring system placed above core cover plate and the helium production rate at this location.

In each experiment, two irradiations were carried out. The short lived foils were irradiated for 8h at 400 kW and retrieved after a cooling time of 24h. The long lived foils were irradiated for 72h at 400 kW and retrieved after 72h of cooling. Details of measurements are given in Ref.14.

4. NEUTRON TRANSPORT CALCULATIONS

Calculations for the experimental shield configurations have been carried out using 2D transport code DORT in X-Y geometry. Calculations have been carried out with DLC-2 100 neutron group cross sections. S_8–P_3 approximation has been used. The Keff convergence was 1.0E-04. The pointwise group flux convergence criterion used is 1.0E-04. This convergence was obtained in all the groups for all the spatial mesh points, but for a few corner points in the first two groups and thermal group.

2D geometry showing various materials from Apsara core to measurement location is given in Fig.5. Reactor core is in the form of rectangular parallelepiped. It's base is 53.78 cm x 53.78 cm and height is 63.5 cm. It consists of 12 (F_{12}), 10(F_{10}), 8(F) and 4 (F_4) plate fuel elements. It also has graphite(G) and beryllium oxide reflector elements. All the fuel elements and reflectors are arranged in a 7x7 square matrix. The fuel elements are homogenised over each square region. Graphite and BeO reflectors at the peripheral positions of the core are also homogenised over the square. The reactor is surrounded by pool water on all sides.

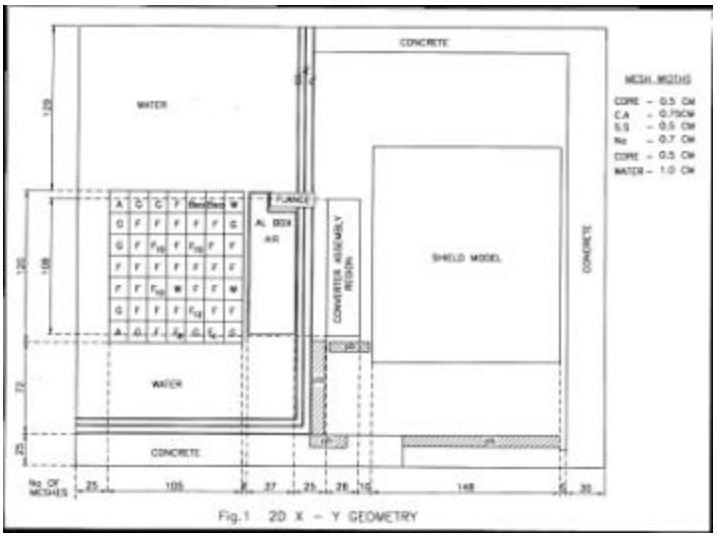

Figure 5. Calculational 2-D Geometry

The wall of reactor pool in shielding corner side consists of SS liner and two Aluminium plates with air between them The water thickness is 4.0 cm and zero cm between the core edge and Al box and Al box and pool liner respectively. The CAs have been modelled as homogeneous assemblies, with volume weighting. The hexagonal outline has been modelled as close as possible in 2D X-Y representation. Activation/fission cross sections in 100 groups were used to calculate reaction rates. The total neutron flux at the core centre was normalised to the total flux obtained using the 3D transport calculations, carried out elsewhere. Details of our calculations are given in Ref.15.

5. EXPERIMENTAL AND CALCULATIONAL RESULTS

5.1 Neutron Transport Studies in Steel-Sodium

Two shield configurations (configurations 1 & 2) with steel-sodium models of 42 cm thickness were studied. This was followed by a 46.2 cm thick sodium model. The volume fraction of steel in first model was higher by 23% and that of sodium was less by 21%. When second model was replaced by first model,

(i) the fast neutron flux (corresponding to $In^{115}(n,n')In^{115m}$ indium and $Ni^{58}(n,p)Co^{58}$ reaction rates) decreased by a factor of two, due to increased steel volume fraction;

(ii) the epithermal flux (corresponding to Cd-covered $Au^{197}(n,\gamma)Au^{198}$, $Na^{23}(n,\gamma)Na^{24}$ and $Cu^{63}(n,\gamma)Cu^{64}$ reaction rates) did not show significant change and

(iii) the thermal flux (corresponding to bare $Au^{197}(n,\gamma)Au^{198}$, $Na^{23}(n,\gamma)Na^{24}$ and $Cu^{63}(n,\gamma)Cu^{64}$ reaction rates) decreased by 20 to 30%, due to decreased sodium volume fraction.

Neutron transport calculations carried out for these experimental configurations showed similar trends. However the magnitude of attenuation was higher by 20 to 50% in the case of reaction rates, sensitive to thermal and epithermal neutrons. Reaction rates, sensitive to fast neutrons (above 2 MeV), were predicted within 20%.

5.2 Neutron Transport Studies in Steel-Sodium-borated Graphite and Steel-Sodium-boron Carbide

To study the effectiveness of borated materials as neutron shields, two configurations were studied. The configuration-3 consisted of 45 cm thick steel-sodium model , followed by 49.5 cm thick steel-sodium-borated graphite model, with four layers of 7.0 cm thick borated graphite and

46.2 cm thick sodium model. In configuration-4, 49.5 cm thick steel-sodium-borated graphite model was replaced by 49.5 cm thick steel-sodium-boron carbide model, with three layers of 9.3 cm thick boron carbide. The reaction rates at 68 cm distance from the incident face were compared.

When borated graphite was replaced by boron carbide, (i) the fast neutron flux (corresponding to $In^{115}(n,n')In^{115m}$ indium and $Ni^{58}(n,p)Co^{58}$ reaction rates) decreased by a factor of two to three,

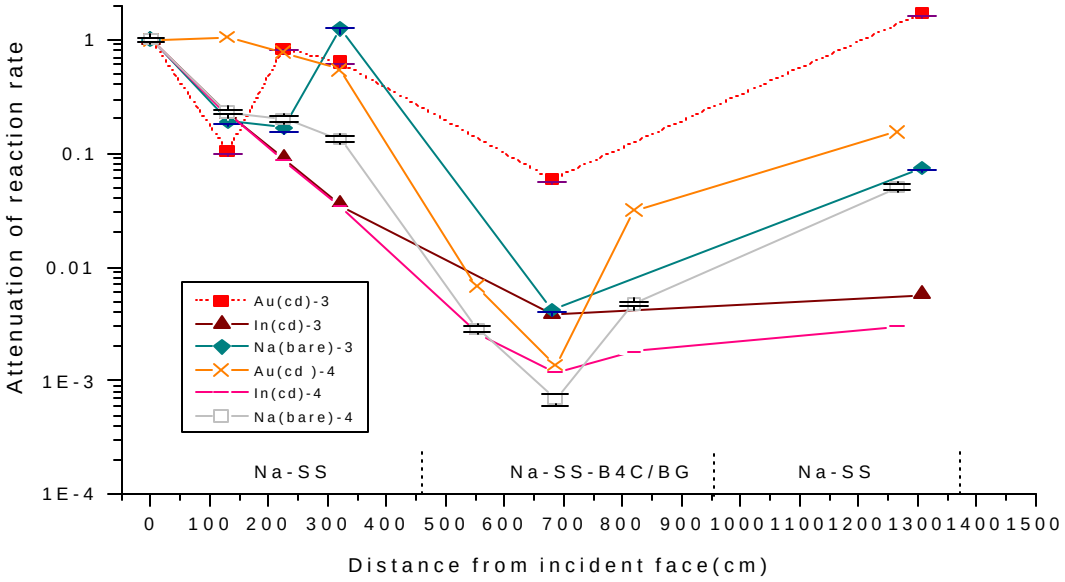

Figure 6. Attenuation in Steel-Borated graphite/Boron Carbide-sodium Shields

(ii) the epithermal fux (corresponding to Cd-covered $Au^{197}(n,\gamma)Au^{198}$, $Na^{23}(n,\gamma)Na^{24}$ and $u^{63}(n,\gamma)Cu^{64}$ reaction rates) decreased by a factor of 20 and (iii) the bare $Na^{23}(n,\gamma)Na^{24}$ reaction rate decreased by a factor of six.

Calculations were carried out with 2-D transport code DORT and DLC-2 cross sections. The attenuation factors and C/E values for typical reaction rates such as, bare $Na^{23}(n,\gamma)Na^{24}$, Cd-covered $Au^{197}(n,\gamma)Au^{198}$, $In^{115}(n,n')In^{115m}$ and $Ni^{58}(n,p)Co^{58}$, are shown in Figs. 6 and 7, for the experiments with borated graphite and boron carbide respectively.

In the calculations of transport through steel/borated graphite/sodium shields, C/E is found to be between 0.35 to 1.6, in the case of thermal and epithermal activation detectors. In the case of threshold detectors, C/E lies between 0.3 to 1.02. The fission equivalent flux above 2.0 MeV is underpredicted by a factor of 2. In the calculations of transport through steel/boron carbide/sodium shields, C/E is found to be between 0.20 to 1.5, in the case of thermal and epithermal activation detectors. In the case of threshold detectors, C/E lies between 0.3 to 1.0. The fission equivalent flux above 2.0 MeV is underpredicted by a factor of 3. It is seen that the calculations underpredict the reaction rates, the extent of underprediction increasing with shield thickness. This is probably due to the presence of strongly absorbing material, boron.

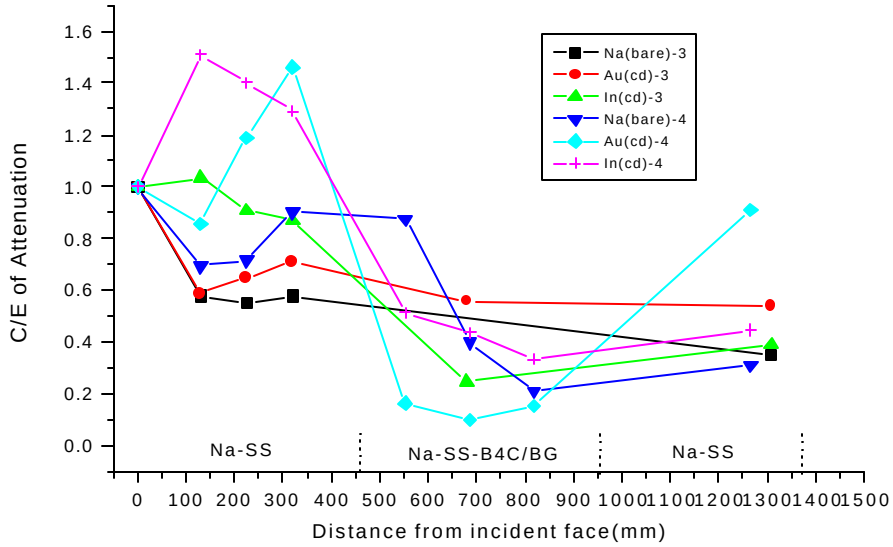

Figure 7. C/E in transport through steel-borated graphite/boron carbide-sodium shields

5.3 Neutron Transport in Steel-Sodium-Graphite and Boron Carbide

From the earlier experiments, it is clear that there is an optimum thickness of boron carbide, beyond which effectiveness of boron is not significant. Hence experiments were carried out with replacing boron carbide by graphite progressively. Experiment-4 corresponds to the case, where only boron carbide is present. In experiment-5, the first 9.3 cm of boron carbide was replaced by 7.3 cm of graphite and 2 cm steel. In experiment-6, the first and the second boron carbide layers were replaced by graphite and steel. Some of the typical attenuation of measured reaction rates along the shield thickness in the three cases are shown in Figs.8, 9 and 10.

To study the effectiveness of replacing graphite by boron carbide, the attenuation in the steel/graphite/boron carbide/sodium model alone was considered (i.e. attenuation in the shield model thickness between 32.0 cm and 81.9 cm). Analysis of the measured reaction rates indicates that 10 cm boron carbide as the last layer of shielding is sufficient to absorb most of the thermalised neutrons. C/E values for typical reaction rates are presented in Table-1 for all the three sets of measurements. It is seen that the calculations underpredict the reaction rates, the extent of underprediction increasing with shield thickness.

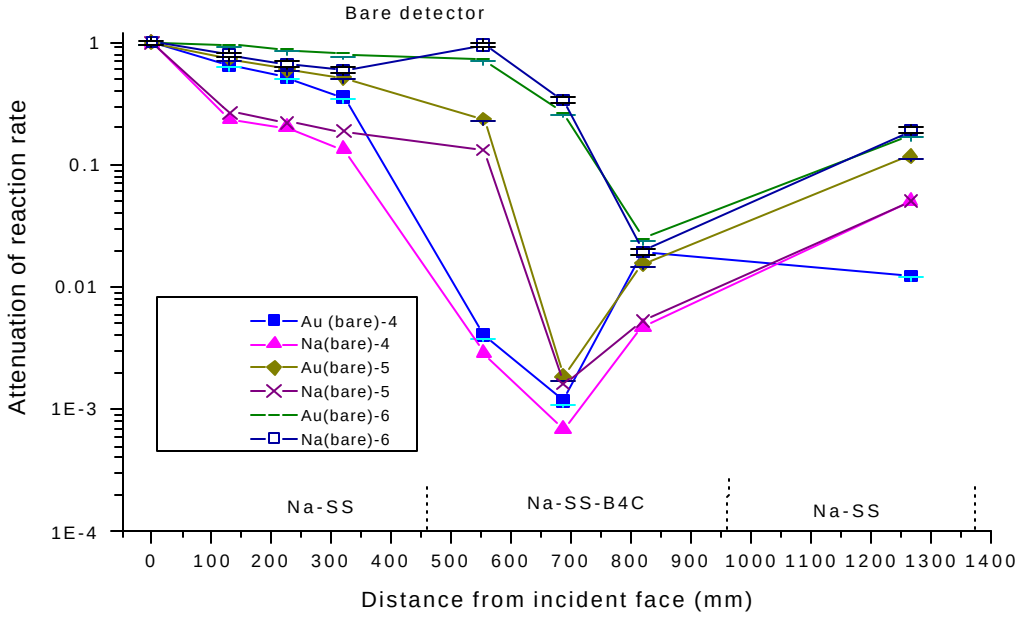

Figure 8. Attenuation of Bare Foil Reaction Rates

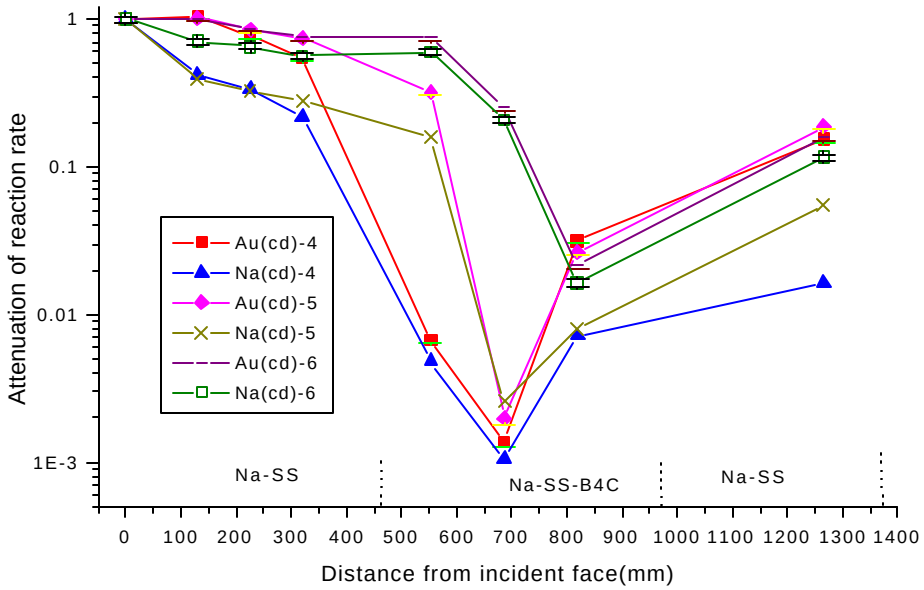

Fig.9 Attenuation of Cd-covered Reaction Rates

Figure 9. Attenuation of Cd-covered Foil Reaction Rates

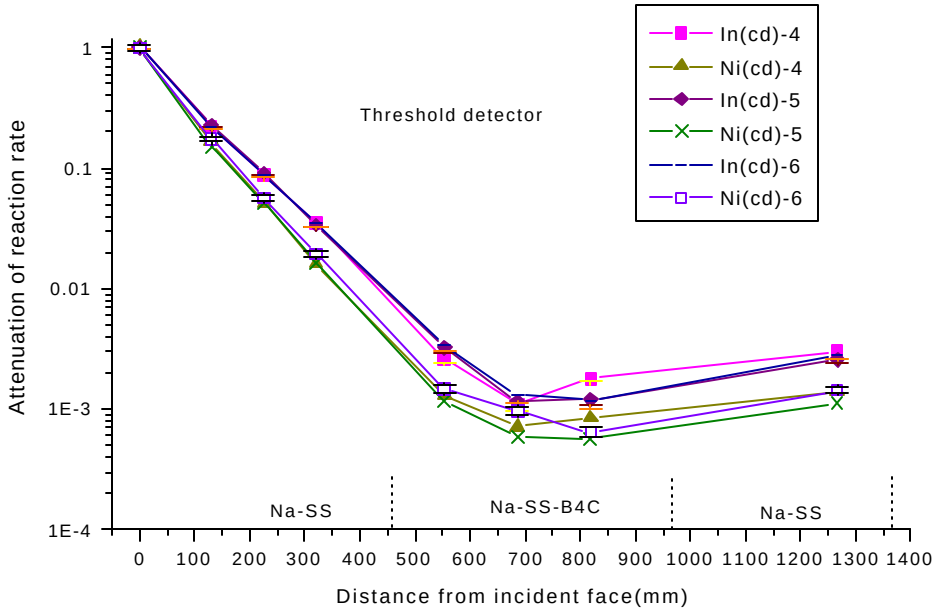

Figure 10. Attenuation of Threshold detector reaction Rates

Table 1. Ratio of calculated to experimental reaction rates

	Experiment-4				Experiment-5				Experiment-6			
Dist-ance	Na (ba)	Au/ Cd	In/ Cd	Ni/ Cd	Na (ba)	Au/ Cd	In/ Cd	Ni/ Cd	Na (ba)	Au/ Cd	In/ Cd	Ni/ Cd
0	1.00	1.00	1.00	1.00	1.00	1.00	1.00	1.00	1.00	1.00	1.00	1.00
130	0.70	0.86	1.51	1.56	0.47	0.71	1.48	1.75	0.90	0.77	1.56	1.58
225	0.72	1.19	1.40	1.48	0.45	0.79	1.35	1.52	0.96	0.91	1.46	1.48
320	0.90	1.46	1.29	1.44	0.45	0.82	1.33	1.46	0.95	0.99	1.37	1.34
553	0.88	1.68	0.51	0.74	0.41	0.80	0.37	0.58	0.73	0.91	0.37	0.49
686	0.40	1.04	0.44	0.66	0.28	0.12	0.39	0.62	0.59	0.74	0.32	0.31
819	0.21	1.54	0.33	0.45	0.17	0.18	0.47	0.61	0.29	0.23	0.50	0.55
1266	0.31	0.91	0.45	0.55	0.30	0.76	0.52	0.67	0.44	0.94	0.53	0.60

5.4 Neutron Transport in axial shields of Steel-Sodium and Graphite

The experiment with configuration-7 corresponding to axial shields, was made up of three models. The first is a 46.5 cm thick steel-sodium model, followed by 40.6 cm thick graphite-steel -sodium model and 29.5 cm thick steel-sodium model. Various reaction rates were measured, as in the case of earlier experiments. In addition, U-235 fission rate and $B^{10}(n,\alpha)$ reaction rate were also measured. The attenuation of the reaction rates is much less compared to

the radial shield models with boron carbide. This is due to the absence of the highly absorbing boron in the shield. Some of the typical attenuation of measured reaction rates along the shield thickness are shown in Fig.11 C/E for the above reaction rates along the shield thickness are shown in Fig.12.

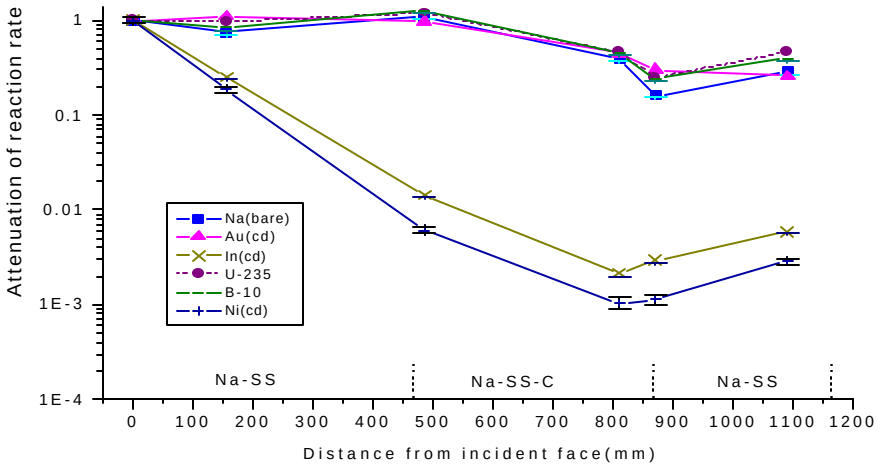

Figure.11. Attenuation of Measured Reaction Rates (Configuration-7)

In the calculations of transport through steel/graphite/sodium shields, C/E is found to be between 0.78 to 1.4, in the case of thermal and epithermal activation detectors. In the case

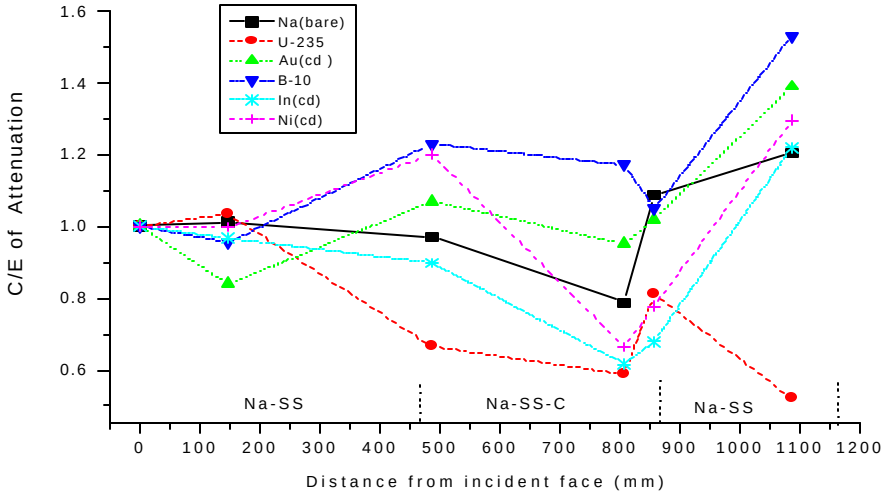

Figure.12. C/E of Attenuation in Reaction Rates (configuration-7)

of threshold detectors, C/E lies between 0.6 to 0.96. The fission equivalent flux above 2.0 MeV is underpredicted by a factor of 2. For bare U^{235}(n,f) reaction rates, C/E lies between 0.52 to 1.03. For bare $B^{10}(n,\alpha)$ reaction rates, C/E lies between 0.96 to 1.53.

The comparison between calculated and measured reaction rates is much better compared to the case, wherein shields with boron carbide/borated graphite were present. All reaction rates are predicted within a factor of two at all locations in the shield models.

6.CONCLUSIONS

Fast reactor shielding facility has been created in the swimming pool thermal reactor APSARA, using depleted uranium assemblies. The neutron flux in the shielding corner has been increased by three orders of magnitude, using an aluminium box filled with air, to replace pool water. Fast reactor shielding mockup experiments have been successfully carried out in the APSARA shielding corner. The measured neutron spectrum incident on the emergent face of CA is close to the expected blanket leakage neutron spectrum of PFBR. In the case of radial shield mockup experiments, analyses of results indicate that 10 cm boron carbide as the last layer of shielding is sufficient to absorb most of the thermalised neutrons. Hence, the initial boron carbide layers can be replaced by graphite, without sacrificing much of shielding efficiency. The choice between graphite and boron carbide for initial layers of shield should be based on cost and engineering considerations.

In the case of transport through steel-sodium shields, calculations predict the fluxes within a factor of two. In the case of radial shields with boron carbide, the calculations generally underpredict the neutron fluxes by a factor of three to five. The sodium reaction rate is underpredicted by a factor of four to five. In the case of mockup experiments for axial shields, calculations predict most of the reaction rates within 20%. Few are predicted within a factor of two. The bare U^{235}(n,f) reaction rate is underpredicted by a factor of two, at the exit of axial shield model. This has helped in the design of neutron detectors on the lattice plate, as large margin could not be provided. Bare $B^{10}(n,\alpha)$ reaction rate is overpredicted by 50%, implying that the calculated value of Helium production rate is on the conservative side. The mockup experiments have been extremely useful in arriving at bias factors to be applied in in-vessel shield design.

ACKNOWLEDGEMENTS

The experiments are a collaborative work between RPD, REG, IGCAR and RPDD, RDDG, BARC. We are thankful to Shri Anil Kakodkar, Chairman, AEC for the encouragement and interest shown in carrying out these experiments. We express our gratitude to Shri. Bhattacharjee, Director, BARC, Shri S.B.Bhoje, Director, IGCAR ,Dr. Om Pal Singh, Head RPD, IGCAR and Shri. R. Srivenkatesan , Head, RPDS, RDDG, BARC for their support. We acknowledge the participation of a large number of persons from IGCAR, BARC and AERB in the design, fabrication, reactor operation and measurement activities.

REFERENCES

[1] J. Butler, Beyond the horizon in Radiation Shielding- A Stochastic world? , Proc. of the Tropical Meeting on New Horizons in Radiation Protection and Shielding, Pasco, 1992.

[2] John Butler, Forty years on: Quo Vadismus? Eighth international Conference on Radiation Shielding, Texas, 1994.

[3] R. Indira, Fast Reactor Shielding- Design Studies and Benchmark Analysis, National Conference on Radiation Shielding and Protection, RASP-96, Kalpakkam,1996.

[4] R.E. Maerker and F.J. Muckenthaler,Neutron Transport Through Sodium, Report ORNL 4880,1974.

[5] D. Calamand and D.Maire, The JASON Experimental Programme to validate B_4C/Steel shield Design, Proc. of VII International Conference on Reactor Shielding, Bournemouth,1988.

[6] I.J. Curl,, D, Calamand, K.I. Muller, The role of the JANUS Experimental Shielding Programme in the Assessment of the Shielding Methods Employed for EFR, Proc. Of the Tropical Meeting on New Horizons in Radiation Protection and Shielding,Pasco,1992,p305.

[7] D.T. Ingersoll and N. Ohtani, JASPER: A joint U.S.- Japan Program of experimental Shielding Research, , Proc. of VII International Conference on Reactor Shielding, Bournemouth,1988.

[8] R. Indira, A.K. Jena et al.,Shielding Benchmark Experiments and Analysis, Proc. Of Workshop on Nuclear Data Evaluation, Kalpakkam, 1981.

[9] R. Indira and K.P.N. Murthy, Monte Carlo Simulation of the Benchmark Experiments on Neutron Transport in Thick Sodium, Report RRC-48,1981.

[10] H.K.Dravid and R. Indira, Bulk Shielding Experiments at APSARA for Prototype Fast Breeder Reactor, BARC Newsletter No.216, January 2002.

[11] W.A. Rhodes and R.L. Childs, DORT- An Updated Version of DOT-4 One and Two Dimensional Neutron/Photon Transport Code, ORNL 5851, 1982.

[12]RSIC Data Library DLC2/100G, 100 Group Neutron Multigroup Cross sections Based on ENDF-B III,1972.

[13]R.Indira, D. Sunilkumar and H.K. Dravid, “Fast Reactor Bulk Shielding Benchmark-Comparison between calculation and measurements at the incident face of shield models”,

Proceedings of Fourteenth National Symposium on Radiation Physics, Amritsar, India, November 1-3, 2001.

[14] H.K. Dravid, R. Indira et.al, Experimental Results of PFBR Radial Bulk Shielding Experiments (set-1 to set-7) at APSARA,Restricted Reports BARC/2001/R/005 to R/008,2001 and BARC/2002/R/007 to R/009,2002.

[15] R.Indira, D. Sunilkumar and H.K. Dravid, PFBR Bulk Shielding Experiments at APSARA (set-1 to set-7)- Comparison of Calculations and Measurements, Restricted Reports PFBR/01115/DN/1077,1078,1083,1084/ 2001 and PFBR/0115/DN/1109 to 1111/2002.